

# Preparation and characterizations of a new PS/TiO<sub>2</sub> hybrid membranes by sol–gel process

Yanan Yang<sup>a,b</sup>, Peng Wang<sup>a,\*</sup>

<sup>a</sup> *Research Center for Green Chemistry and Technology, School of Municipal and Environmental Engineering, Harbin Institute of Technology, Harbin 150090, China*

<sup>b</sup> *Changchun University of Technology, Changchun 130012, China*

Received 5 July 2005; received in revised form 18 November 2005; accepted 10 January 2006

Available online 3 March 2006

## Abstract

New organic–inorganic hybrids based on PS/TiO<sub>2</sub> hybrid membranes were prepared by sol–gel and phase inversion process. The membranes were characterized in terms of morphology, structure, hydrophilicity, UF performance and thermal stability. The results showed that macrovoids were nearly suppressed with formation of a sponge like membrane structure. The TiO<sub>2</sub> particles were uniformly dispersed in membrane. The nanodispersed inorganic network formed after sol–gel process and the strong interaction between inorganic network and polymeric chains led to the improvement of porosity and thermal stability. In particular hydrophilicity and permeability increased drastically with the increasing of TiO<sub>2</sub> content in the range of 0–9.3 wt%, without changing retention properties of membrane. However, high-TiO<sub>2</sub> concentration induces nanoparticles aggregate, resulting in the decline of hydrophilicity and permeability. Thus, PS/TiO<sub>2</sub> hybrid membranes with proper TiO<sub>2</sub> content are desirable to meet some specific requirements in industrial separation.

© 2006 Elsevier Ltd. All rights reserved.

*Keywords:* Polysulphone; Titanium dioxide; Sol–gel process

## 1. Introduction

Currently, polymers are still the main membrane materials in membrane technology with the advantages of good flexibility, toughness, and separation properties. However, a limited chemical, mechanical and thermal resistance restricts their applied scale. As reported in literatures [1,2], ceramics membranes have higher thermal and chemical resistance and longer lifetime, but they are expensive with poor flexibility and low-separation performance. Hybrid materials can combine basic properties of organic and inorganic materials and offer specific advantages for the preparation of artificial membranes with excellent separation performances, good thermal and chemical resistance and adaptability to the harsh environments, as well as film forming ability [3–6]. Thus, organic–inorganic hybrid materials as new membrane materials have attracted more and more attentions. The sol–gel technique is one of the most extensively applied method for preparation of organic–inorganic nanomaterials, which allows the formation of

inorganic frameworks under mild condition and incorporation of minerals into polymers, resulting in an increased chemical, mechanical and thermal stability without obviously decreasing the properties of the polymers [7–9]. Furthermore, the remained hydrogen bond clusters at the surfaces of the materials after the sol–gel reaction improves the membrane hydrophilicity and enhances hybrid material stability [10–16].

Polysulfone (PS) is one of the most extensively applied ultrafiltration (UF) membrane materials in industry area for mechanical strength, compaction-resistance, chemical stability, thermal resistance and in wide pH value range application (2–12). But its hydrophobic nature is also well-known, which results in the adsorption and deposition of hydrophobic solute on the membrane surface [17]. The adsorption and deposition can cause severe membrane fouling due to the formation of thick gel-layer and the block of the pores, which will result in the flux decline and short-life of membrane. Although the modification of PS have been widely explored such as the modification of membrane surface [18] and membrane material [19], the problems such as tradeoff between permeability and selectivity, the process complexity, the manufacturing costs and stability still remain to be unsolved. Titanium dioxide (TiO<sub>2</sub>) has been the focus of numerous investigations for innocuity, resisting and

\* Corresponding author. Tel.: +86 451 86283801; fax: +86 451 82603898.  
E-mail address: [pwang73@vip.sina.com](mailto:pwang73@vip.sina.com) (P. Wang).

decomposing bacterias, UV-proof and super hydrophilicity [20] in recent years. Therefore, it has been applied to a variety of problems of environmental interest in addition to water and air purification [21].

The aim of this work was to prepare a novel PS/TiO<sub>2</sub> organic–inorganic hybrid UF membrane with high hydrophilicity and permeability, mechanical and thermal stability by sol–gel and phase inversion process. The preparation of PS/TiO<sub>2</sub> hybrid membranes with finely dispersed TiO<sub>2</sub> in the polymer matrix was discussed. The effects of existence of TiO<sub>2</sub> nanoparticles and resulting in organic framework on membranes properties were investigated by examining UF performances, hydrophilicity, thermal analysis of membranes, as well as the microstructures of membrane.

## 2. Experimental

### 2.1. Materials

PS (S180) was purchased from Shanghai Shupeng, China. Polyvinylpyrrolidone (PVP, K30) was obtained from BASF, Germany. *N,N'*-Dimethylacetamide (DMAc), *N*-methyl-2-pyrrolidinone (NMP), tetrabutyltitanate (Ti (OBu)<sub>4</sub>), were obtained from Shanghai Chemical Reagent Company (China) and used without further purification. Acetate acid and hydrochloric acid (HCl, 36–38%) were of analytical grade (from Beijing Chemical Reagent Company, China) and used as received. The Bovine serum albumin (BSA, 67 kDa) was purchased from Beijing Dingguo Biologic Tech (China).

### 2.2. TiO<sub>2</sub> sol preparation

1.0 mL acetate acid and 10.0 mL Ti(OBu)<sub>4</sub> were added to 10.0 mL NMP with stirring (solution A). 0.3 mL HCl in 2.0 mL deionized water was added to another 10.0 mL NMP (solution B). Then solution B was added dropwise to solution A with vigorous stirring for 2 h at room temperature. After mixing uniformly, stable, transparent and flaxen TiO<sub>2</sub> sol was obtained with pH 4.0 adjusted by HCl.

### 2.3. Membrane preparation

TiO<sub>2</sub> sol with different content (0, 1.3, 3.3, 5.3, 7.3, 9.3, 11.9, 14.6, and 17.2 wt%) was added dropwise to the casting solution of DMAc and NMP (vol<sub>DMAc</sub>:vol<sub>NMP</sub> = 4:1) containing 18 wt% PS and 4 wt% additive PVP with constant stirring for 24 h. The above mixture solution was evacuated for 24 h to remove air bubbles and then was poured onto a glass plate with a doctor blade (thickness: 200 μm) at room temperature. After exposed in air for 10 s, the casting solution on glass was immediately immersed in the ethanol/water (20:80 in volume) bath. The resulting membrane was transferred to a room-temperature water bath and stand for 1–2 days to remove off the remaining solvent and make Ti (OBu)<sub>4</sub> hydrolyzed fully. The membrane was stored in demineralized water containing 1% formaldehyde to avoid bacteria growth.

### 2.4. Membrane characterizations

#### 2.4.1. Morphology observation

Membrane surfaces and cross sections are observed by means of JSM-5500 LV scanning electron microscope (SEM, Japan electron). All specimens were freeze–dried and coated with a thin layer of gold before observation. Cross-section was prepared by fracturing the membranes in liquid nitrogen.

#### 2.4.2. Porosity calculation and the X-ray diffraction (XRD) analysis

Porosity (Pr, %) was calculated as a function of the membrane weight.

$$\text{Pr} = \frac{W_w - W_d}{S d d_m} \times 100\%$$

$W_w$  and  $W_d$ , weights of membrane at equilibrium swelling with water and at dry state, respectively,  $S$  the area of the membrane,  $d$  the average thickness of the membrane,  $d_m$  the density of water.

The membrane XRD patterns were recorded on a D/max-rB diffractometer (Japan) equipped with graphite monochromated Cu K $\alpha$  radiation ( $\lambda = 0.15405$  nm) operated at 50 mA and 50 kV from 10 to 80°.

#### 2.4.3. UF performances and hydrophilicity

The water permeability of the membranes was measured with an SCM 300 ultrafiltration cup (ecologic center, Shanghai) fed with demineralized water for 15 min. The test was repeated until the water permeability remaining constant. The retention was described as molecular weight of BSA. The tests were also carried out with an SCM 300 ultrafiltration cup fed with an aqueous solution of BSA (100 mg/mL) for 15 min. Operating conditions were: room temperature, transmembrane pressure of 1 bar and a tangential water velocity of 3 m/s. The contact angle between water and the membrane surface was measured to evaluate the membrane hydrophilicity, using a DSA 10-MK2 contact angle goniometer (KRÜSS, Germany). To minimized experimental error, the contact angles were measured 8 times for each sample and then were averaged.

#### 2.4.4. Thermal analysis

The thermal stability of hybrid membranes was evaluated by thermogravimetric analysis (TGA, Perkin–Elmer Pyris Diamond). The TGA measurements were carried out under nitrogen atmosphere at a heating rate of 10 °C from 50 to 800 °C. Differential scanning calorimetry (DSC, Perkin–Elmer DSC7) measurements were performed on the hybrid membranes from 50 to 300 °C at a heating rate of 10 °C. The first scan was run to 300 °C for 10 min to destroy any initial thermal history, and then the samples was cooled to 50 °C to start the second scan.

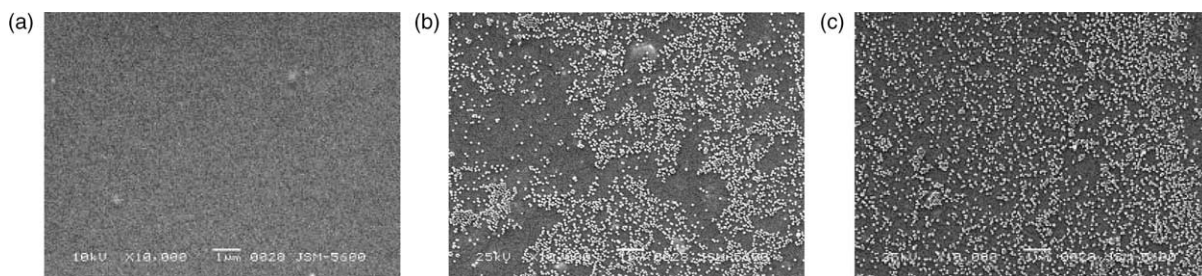


Fig. 1. SEM pictures of PS/TiO<sub>2</sub> composite membranes with different TiO<sub>2</sub> concentration: (a) 0 wt%, (b) 5.3 wt%, (c) 7.3%.

### 3. Results and discussion

#### 3.1. Membrane morphology

The morphologies of PS and PS/TiO<sub>2</sub> membranes were observed by SEM. Fig. 1 shows that there are an amount of TiO<sub>2</sub> nanoparticles packed by polymers or aggregates of TiO<sub>2</sub>

nanoparticles adsorbing or embedding on the surface of PS/TiO<sub>2</sub> hybrid membrane (Fig. 1(b) and (c)) compared with PS membrane (Fig. 1(a)). This phenomena indicates that the drastic increase in casting solution viscosity caused by addition of TiO<sub>2</sub> sol and the interaction caused by adsorption between TiO<sub>2</sub> and polymers lead to nanoparticles move difficultly and adsorbed or embed in the skinlayer.

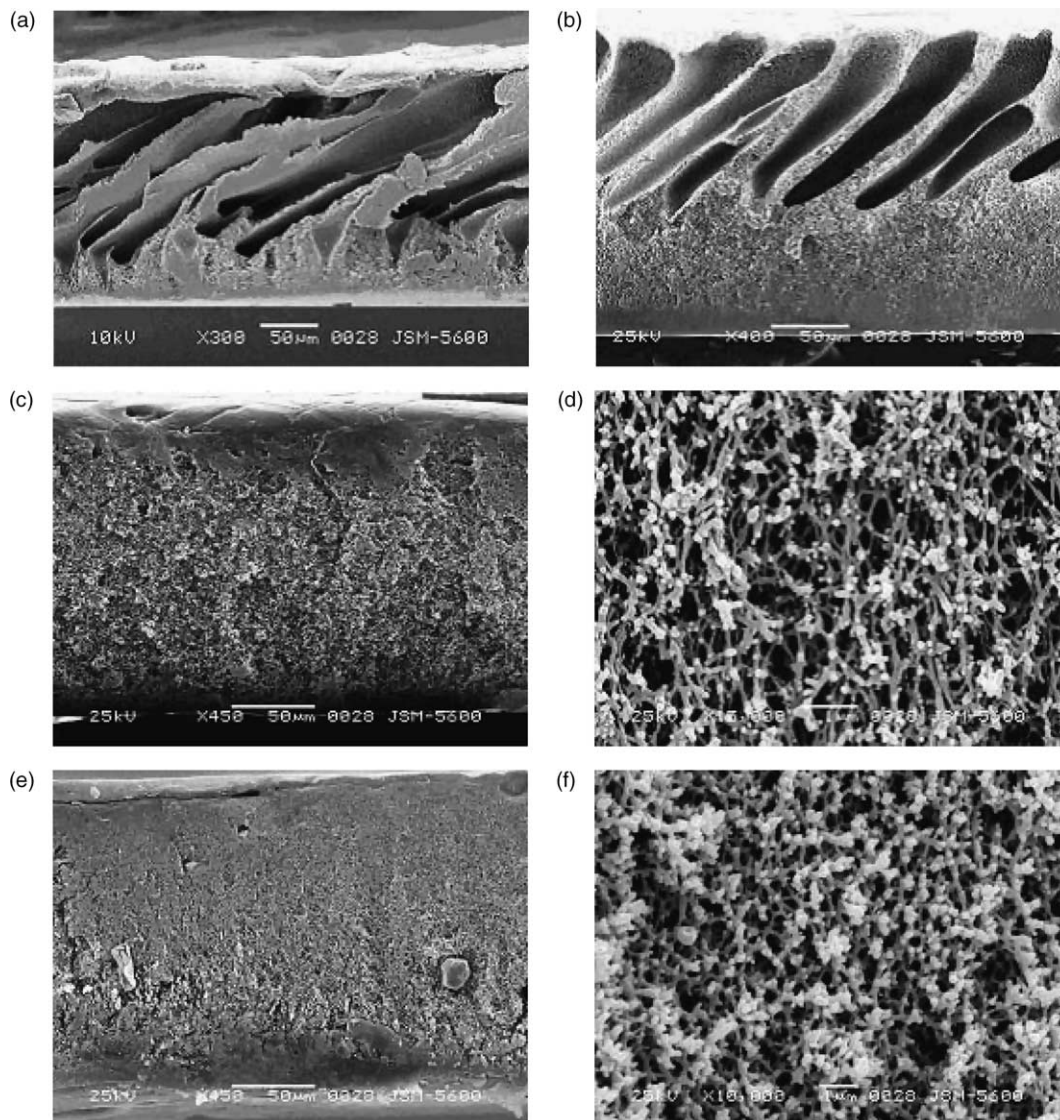


Fig. 2. SEM micrographs of cross-section of PS/TiO<sub>2</sub> membranes with different TiO<sub>2</sub> concentration: (a) 0 wt%, (b) 3.3 wt%, (c) 9.3 wt%, (d) c's local magnifying figure, (e) 14.6 wt%, (f) e's local magnifying figure.

Table 1  
Porosity of PS/TiO<sub>2</sub> hybrid membrane with different TiO<sub>2</sub> content

TiO <sub>2</sub> concentration (wt%)	Porosity (%)
0	42.9
3.3	77.5
9.3	84.7
14.6	86.3

Fig. 2 shows that with the increase in the TiO<sub>2</sub> concentration, the topical asymmetric structure of membrane (Fig. 2(a)) becomes faint, the thickness of skinlayer increases (Fig. 2(b)) and the structure of sublayer undergoes a transition from finger like to sponge like structure (Fig. 2(c)). The increase in the viscosity of the casting solution due to the addition of TiO<sub>2</sub> sol slows down the exchange rate of solvent (DMAc/NMP)/nonsolvent (ethanol/water) and results in a delayed demixing process, with macrovoids suppression [22]. According to the hypothesis of McKelvey and Koros [22], macrovoids are initiated by nucleation of the polymer-lean phase just beneath the skinlayer, and its growth lies on the rate difference between the indiffusion rate of nonsolvent to casting solution and the diffusion rate of the solvent to coagulation bath. This rate difference induces a nonsolvent concentration gradient in casting solution, which forms a drive force to cause the macrovoids growth. With the increase in casting solution viscosity induced by addition of TiO<sub>2</sub> sol, the diffusion of nonsolvent slows down greatly and nonsolvent concentration decreases. Consequently, the formation or the growth of macrovoids in membranes is suppressed, and a sponge like structure with entrapped TiO<sub>2</sub> particles is formed (Fig. 2(d)) [23–27]. So, PS/TiO<sub>2</sub> hybrid membranes present a morphology with decreased or eliminated macrovoids, and as consequences, an increase in resistance and mechanical strength.

### 3.2. Porosity and XRD analyses

The porosity of the membrane is shown in Table 1 and in the magnification of sublayer membrane (Fig. 3), respectively. Shrinkage of organic phase during the precipitation process of wet-casting polymeric membranes builds up stress between polymer and TiO<sub>2</sub>, with consequent formation of pores. Fig. 4 shows the XRD diffraction patterns of TiO<sub>2</sub> nanoparticles, PS membrane and PS/TiO<sub>2</sub> hybrid membrane. The pattern of TiO<sub>2</sub> crystal powder has three crystalline characteristic peaks at  $2\theta$

25.32, 37.86 and 48.06°, which agree with the literature report [28], and the pattern of hybrid membrane has also three crystalline characteristic peaks at  $2\theta$  of 28.06, 38.76, and 48.1° that is analogous with the characteristic peaks of TiO<sub>2</sub> crystal powder in addition to the dispersion peak of amorphous PS. This indicates that tetrabutyltitanate has formed TiO<sub>2</sub> crystal through hydrolytic reaction during the preparation of PS/TiO<sub>2</sub> hybrid membrane.

### 3.3. Membrane hydrophilicity and UF performances

#### 3.3.1. The hydrophilicity of membranes

The contact angle data of PS/TiO<sub>2</sub> hybrid membranes with different TiO<sub>2</sub> concentration listed in Table 2 shows that the membrane hydrophilicity is improved by addition of TiO<sub>2</sub> sol. This fact is due to the presence of TiO<sub>2</sub> nanoparticles generated by tetrabutyltitanate hydrolysis containing an amount of hydroxyl groups, responsible of the hydrophilicity increase. However, the contact angle increases when TiO<sub>2</sub> concentration is over 11.9 wt% due to nanoparticles aggregate, resulting in decreasing of hydroxyl groups number. After 15 days of immersion in water bath, the hydrophilicity is highly maintained with the same trend, due to the strong interactions between TiO<sub>2</sub> and polymers.

#### 3.3.2. UF performance of membranes

The influence of TiO<sub>2</sub> concentration on permeability and retention is investigated through UF experiments. Fig. 5 shows that the membrane permeability increases with the concentration of TiO<sub>2</sub>, with a peak value at 9.3 wt%. However, higher TiO<sub>2</sub> concentration leads to the decrease in permeability. An increase in porosity and hydrophilicity of membrane enhances greatly the permeability greatly. However, high-TiO<sub>2</sub> sol concentration produces highly viscous casting solution which slows down the formation process of hybrid membrane and causes to form a thicker skinlayer and a compact network sublayer containing considerable TiO<sub>2</sub> particles blocking membrane pores and thereby producing a negative effect on permeability. It should be noted that retention of hybrid membrane about BSA kept almost unchanged compared to the PS membrane (Fig. 5) owing to the balance between porosity increase and compact structure of organic–inorganic network.

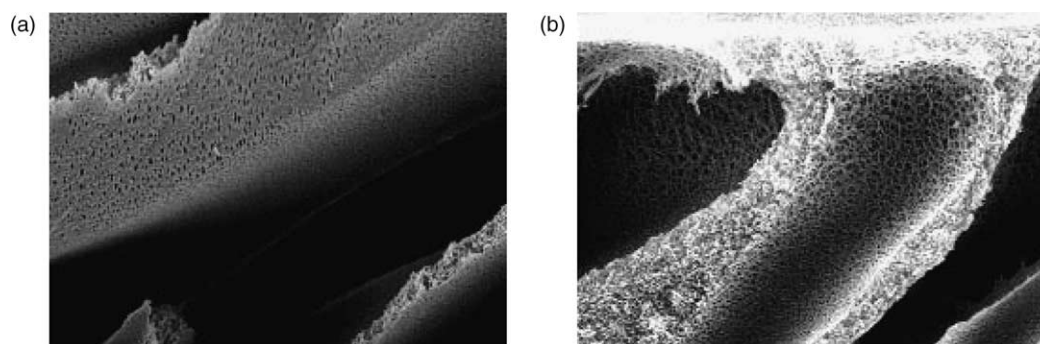


Fig. 3. The SEM images of the pore density of PS membrane (a) and PS/TiO<sub>2</sub> hybrid membrane with 3.3 wt% TiO<sub>2</sub> (b).

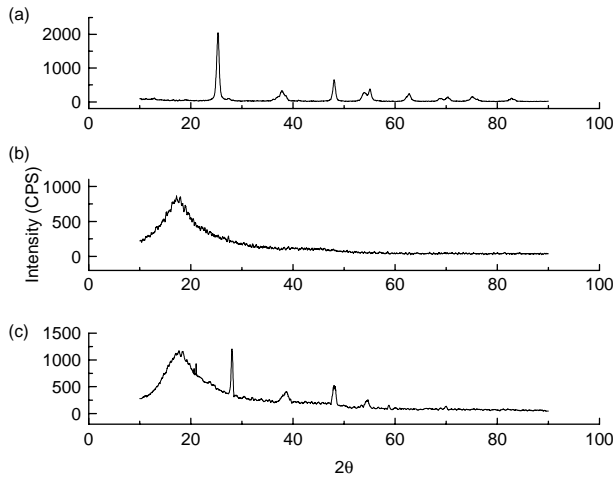


Fig. 4. X-ray diffraction patterns of TiO<sub>2</sub> powder (a) PS membrane (b) and PS/TiO<sub>2</sub> hybrid membrane (c).

Table 2  
Contact angle of PS/TiO<sub>2</sub> hybrid membranes with different TiO<sub>2</sub> content

Sample number	TiO <sub>2</sub> concentration (wt%)	Contact angle (°)
1	0	87.7
2	1.3	76.2
3	3.3	64.7
4	5.3	50.6
5	7.3	41.3
6	9.3	32.2
7	11.9	38.4
8	14.6	43.1
9	17.2	49.7

Thus, PS/TiO<sub>2</sub> hybrid membranes possess superior permeability and unchanged retention.

### 3.4. Thermal properties

The thermal analysis results of PS/TiO<sub>2</sub> hybrid membrane are illustrated in Figs. 6 and 7, respectively. It can be seen that the decomposing temperature ( $T_d$ , defined as the temperature

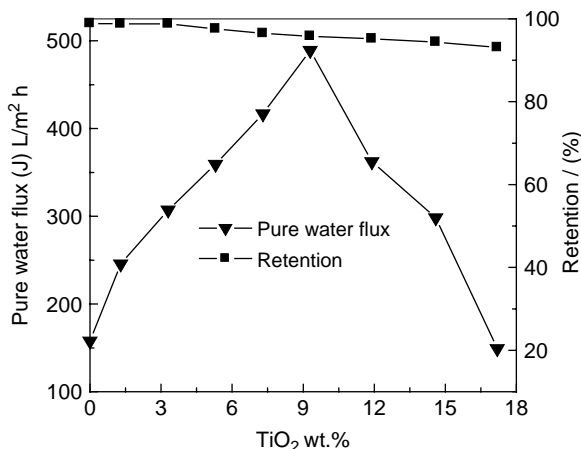


Fig. 5. Pure water flux and retention of PS/TiO<sub>2</sub> hybrid membranes as a function of TiO<sub>2</sub> concentration.

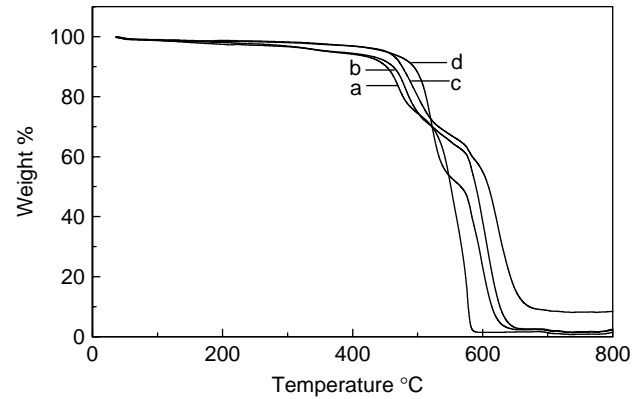


Fig. 6. TG curves of PS/TiO<sub>2</sub> hybrid membranes with different TiO<sub>2</sub> content: (a) 0 wt%,  $T_d$  471.95 °C; (b) 5.3 wt%,  $T_d$  481.22 °C; (c) 9.3 wt%,  $T_d$  496.02 °C; (d) 17.2 wt%,  $T_d$  522.37 °C.

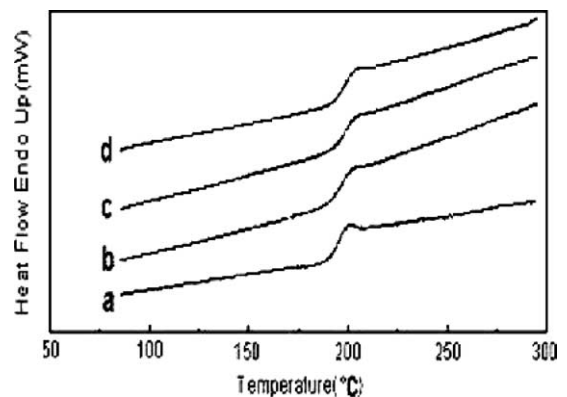


Fig. 7. DSC thermograms of PS/TiO<sub>2</sub> composite membrane versus TiO<sub>2</sub> concentration: (a) 0 wt%,  $T_g$  185.02 °C; (b) 5.3 wt%,  $T_g$  188.36 °C; (c) 9.3 wt%,  $T_g$  191.48 °C; (d) 17.2 wt%,  $T_g$  198.23 °C.

at 3% weight loss) and  $T_g$  of hybrid membrane increase with the increasing of TiO<sub>2</sub> content reaching at 17.2 wt% the highest values:  $T_d$  and  $T_g$  are enhanced of 54.2 and 13.21 °C, respectively, compared with polymeric membrane. We can reasonably conclude that interaction of hydrogen bond or other coordinate bonds between TiO<sub>2</sub> inorganic network formed after sol–gel process and polymeric chains, restrict the thermal action of macromolecules, increasing the rigidity of macromolecular chain and enhancing the energy needed by polymeric chain movement and breakage.

## 4. Conclusions

New organic–inorganic PS/TiO<sub>2</sub> hybrid membranes were prepared by sol–gel and phase inversion process. The microstructure, porosity, hydrophilicity, UF performance and thermal stability of hybrid membrane are improved apparently by an appropriate choice of TiO<sub>2</sub> concentration. The main conclusions from the results of this study were listed as follows:

1. Macrovoids are restricted and eliminated, the topical asymmetric structure of membrane becomes faint and undergoes a transition from macrovoids to network pores,

consequently the compact resistance of membrane is enhanced.

2. A net structure with inorganic network impenetrating with polymeric networks each other and TiO<sub>2</sub> particles as cross-linking spots after sol–gel process is formed due to the interaction of hydrogen bond or other coordinate bond between TiO<sub>2</sub> inorganic network and polymeric chains, as morphology and excellent thermal properties of hybrid membranes prove.
3. The hybrid membranes exhibit extraordinary hydrophilicity, increased porosity and superior permeability with unchanged retention properties in contrast with polymeric membranes.

## References

- [1] Clarizia G, Algieri C, Drioli E. Filler–polymer combination: a route to modify gas transport properties of a polymeric membrane. *Polymer* 2004; 45:5671–81.
- [2] Guizard C, Burggraaf AJ. In: Burggraaf AJ, Cot L, editors. *Fundamentals of inorganic membrane science and technology*. Amsterdam: Elsevier; 1996. p. 227–59.
- [3] Guizard C, Bac A, Barboiu M, Hovnanian N. Hybrid organic–inorganic membranes with specific transport properties. Applications in separation and sensors technologies. *Sep Purif Technol* 2001;25:167–80.
- [4] Chiang PC, Whang WT, Tsai MH, Wu SC. Physical and mechanical properties of polyimide/titania hybrid films. *Thin Solid Films* 2004; 447/448:359–64.
- [5] Taniguchi A, Cakmak M. The suppression of strain induced crystallization in PET through sub micron TiO<sub>2</sub> particle incorporation. *Polymer* 2004;45:6647–54.
- [6] Lua ZH, Liu GJ, Duncan S. Poly(2-hydroxyethyl acrylate-co-methyl acrylate)/SiO<sub>2</sub>/TiO<sub>2</sub> hybrid membranes. *J Membr Sci* 2003;221: 113–22.
- [7] Zhang JZ, Li B, Wang ZX, Dong SJ. Functionalized inorganic–organic composite material derived by sol–gel for construction of mediated amperometric hydrogen peroxide biosensor. *Anal Chim Acta* 1999;388: 71–8.
- [8] Neoh KG, Tan KK, Goh PL, Huang SW, Kang ET, Tan KL. Electroactive polymer–SiO<sub>2</sub> nanocomposites for metal uptake. *Polymer* 1999;40: 887–94.
- [9] Cho JW, Sul KI. Characterization and properties of hybrid composites prepared from poly(vinylidene fluoride–tetrafluoroethylene) and SiO<sub>2</sub>. *Polymer* 2001;42:727–35.
- [10] Nagarale RK, Shahi VK, Rangarajan R. Preparation of polyvinyl alcohol-silica hybrid heterogeneous anion-exchange membranes by sol–gel method and their characterization. *J Membr Sci* 2005;248:37–44.
- [11] Kim DS, Park HB, Rhim JW, Lee YM. Preparation and characterization of crosslinked PVA/SiO<sub>2</sub> hybrid membranes containing sulfonic acid groups for direct methanol fuel cell applications. *J Membr Sci* 2004;240: 37–48.
- [12] Clarizia G, Algieri C, Drioli E. Filler–polymer combination: a route to modify gas transport properties of a polymeric membrane. *Polymer* 2004; 45:5671–81.
- [13] Wu CM, Xu TW, Yang WH. Fundamental studies of a new hybrid (inorganic–organic) positively charged membrane: membrane preparation and characterizations. *J Membr Sci* 2003;216:269–78.
- [14] Zhong SH, Li CF, Xiao XF. Preparation and characterization of polyimide-silica hybrid membranes on kieselguhr-mullite supports. *J Membr Sci* 2002;199:53–8.
- [15] Kim JH, Lee YM. Gas permeation properties of poly(amide-6-*b*-ethylene oxide)-silica hybrid membranes. *J Membr Sci* 2001;193:209–25.
- [16] Honma I, Hiraoka S, Yamada K, Bae JM. Synthesis of organic/inorganic nanocomposites protonic conducting membrane through sol–gel processes. *Solid State Ionics* 1999;118:29–36.
- [17] Ramesh Babu P, Gaikar VG. Membrane characteristics as determinant in fouling of UF membranes. *Sep Purif Technol* 2001;24:23–34.
- [18] Gancarz I, zniak GP, Bryjak M, Tylus W. Modification of polysulfone membranes 5. Effect of *n*-butylamine and allylamine plasma. *Eur Polym J* 2002;38:1937–46.
- [19] Yoo JE, Kim JH, Kim Y, Kim CK. Novel ultrafiltration membranes prepared from the new miscible blends of polysulfone with poly(1-vinylpyrrolidone-co-styrene) copolymers. *J Membr Sci* 2003;216: 95–106.
- [20] Liu P, Lin HX, Fu XZ, et al. Preparation of the doped TiO<sub>2</sub> film photocatalyst and its bactericidal mechanism. *Chin J Catal* 1995;20(3): 327–8 (Ch).
- [21] Hoffmann MR, Martin ST, Choi W, Bahnemann DW. Environmental application of semiconductor photocatalysis. *Chem Rev* 1995;95:69–75.
- [22] McKelvey SA, Koros WJ. Phase separation, vitrification and the manifestation of macrovoids in polymeric asymmetric membranes. *J Membr Sci* 1996;112:29–39.
- [23] Hu Q, Marand E. In situ formation of nanosized TiO<sub>2</sub> domains within poly(amide–imide) by a sol–gel process. *Polymer* 1999;40:4833–42.
- [24] Kim SH, Kwak SY, Sohn BH, Park TH. Design of TiO<sub>2</sub> nanoparticle self-assembled aromatic polyamide thin-film-composite (TFC) membrane as an approach to solve biofouling problem. *J Membr Sci* 2003;211:157–65.
- [25] Xiong SX, Wang Q, Xia HS. Template synthesis of polyaniline/TiO<sub>2</sub> bilayer microtubes. *Synth Met* 2004;146:37–42.
- [26] Ebert K, Fritsch D, Koll J, Tjahjaviguna C. Influence of inorganic fillers on the compaction behaviour of porous polymer based membranes. *J Membr Sci* 2004;233:71–8.
- [27] Matějka L, Dukh O, Kamišová H, et al. Block-copolymer organic–inorganic networks. Structure, morphology and thermomechanical properties. *Polymer* 2004;45:3267–76.
- [28] Wu FQ, Ruan SP, Li XP, et al. Synthesis, characterization and photocatalytic degradation properties of TiO<sub>2</sub> nanocrystalline. *J Funct Mater* 2001;32(1):69–74 [Chin].